General Upper Bounds on Fluctuations of Trajectory Observables

George Bakewell-Smith,[1] Federico Girotti,[1,2,3] Mădălin Guţă,[1,2] and Juan P. Garrahan[4,2]
[1]School of Mathematical Sciences, University of Nottingham, Nottingham NG7 2RD, United Kingdom
[2]Centre for the Mathematics and Theoretical Physics of Quantum Non-Equilibrium Systems, University of Nottingham, Nottingham NG7 2RD, United Kingdom
[3]Department of Mathematics, Polytechnic University of Milan, Milan, Piazza Leonardo da Vinci 32, 20133, Italy
[4]School of Physics and Astronomy, University of Nottingham, Nottingham NG7 2RD, United Kingdom

(Received 20 December 2022; accepted 21 September 2023; published 8 November 2023)

Thermodynamic uncertainty relations (TURs) are general *lower bounds* on the size of fluctuations of dynamical observables. They have important consequences, one being that the precision of estimation of a current is limited by the amount of entropy production. Here, we prove the existence of general *upper bounds* on the size of fluctuations of any linear combination of fluxes (including all time-integrated currents or dynamical activities) for continuous-time Markov chains. We obtain these general relations by means of concentration bound techniques. These "inverse TURs" are valid for all times and not only in the long time limit. We illustrate our analytical results with a simple model, and discuss wider implications of these new relations.

DOI: 10.1103/PhysRevLett.131.197101

Introduction.—Thermodynamic uncertainty relations (TURs) refer to general *lower bounds* on the size of fluctuations in the observables of trajectories of stochastic systems. TURs were initially postulated as a bound on the variance of time-averaged currents in the stationary state of continuous-time Markov chains [1], and then proven (via "level 2.5" large deviation methods [2–4]) to apply to the whole probability distribution [5]. TURs were then generalized to other dynamics and observables, including finite times [6,7], discrete-time Markov dynamics [8], first-passage times [9,10], and open quantum systems [11–14], among many other extensions and alternative derivations (see, e.g., [15–25]). For a review see Ref. [26].

The most studied TUR is that for the relative uncertainty (variance over mean squared) of a time-integrated current bounded by (twice) the inverse of the entropy production. This has immediate consequences for inference and estimation [1,26]: increased precision in the estimation of the value of a current from a stochastic trajectory requires increasing the dissipation, or alternatively, the value of the entropy production can be inferred from the fluctuations of one or more specific currents which might be easier to access. Similar uses of the TUR can be formulated using the dynamical activity [27–29] for the estimation of time-symmetric observables [9,26].

Despite their success and generality, a limitation of TURs is that they only provide lower bounds on the size of fluctuations: except in the few cases where they are tight, inference on the observable of interest is hindered by the absence of a corresponding upper bound. Here, we correct this issue by introducing a class of general upper bounds for fluctuations of trajectory observables consisting of linear combination of fluxes of a continuous-time Markov chain, which includes all currents and activities. For lack of a better name, we call these "inverse thermodynamic uncertainty relations." The inverse TURs are valid for all times and bound fluctuations at all levels. Figure 1 illustrates our results (see below for details): the large deviation rate function $I(A/t)$ for a current A is upper bounded by the TUR, as known, and lower bounded by our inverse TUR. Below we prove these general relations using spectral and perturbation techniques that are widely applied in the field of quantum and classical Markov processes (see Refs. [30–35] and references therein).

Notation and definitions.—Let $\mathbf{X} \coloneqq (X_t)_{t\geq 0}$ be a continuous-time Markov chain taking values in the finite state space E with generator $\mathbb{W} = \sum_{x\neq y} w_{xy}|x\rangle\langle y| - \sum_x w_{xx}|x\rangle\langle x|$, with $x, y \in E$; we adopt the convention of having $\mathbb{W}$ acting from the right on probability measures on E. If X_0 is distributed according to some measure ν, we denote by $\mathbb{P}_\nu$ the law of $\mathbf{X}$ and we use $\mathbb{E}_\nu$ for the corresponding expected value. We assume that $\mathbf{X}$ is irreducible with unique invariant measure (i.e., stationary state) π. We are interested in studying fluctuations of observables of the trajectory $\mathbf{X}$ of the form

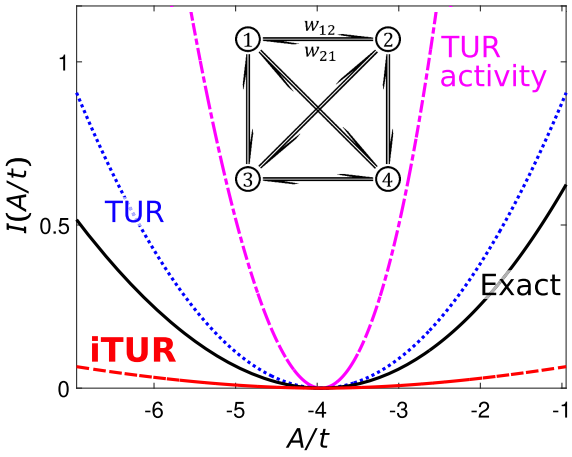

FIG. 1. Upper bound on current fluctuations. The full (black) curve shows the exact rate function $I(A/t)$ for the current defined by $a_{12} = 0.9$, $a_{13} = -0.9$, $a_{14} = -0.9$, $a_{23} = 0.9$, $a_{24} = -0.9$, and $a_{34} = 0.9$. The rate function is upper bounded by the TURs: the dotted (blue) curve is the standard TUR using the entropy production, while the dot-dashed (pink) curve is the TUR with the dynamical activity. The dashed (red) curve is the inverse TUR: it lower bounds the rate function, corresponding to an upper bound on fluctuations at all orders. [We plot the iTUR from a parametric Legendre transform of $\tilde{\Lambda}(u)$ in Eq. (8) to avoid the approximation used to obtain Eq. (3); however, the explicit Eq. (3) gives a very similar bound.] Inset: sketch of the four-state model.

$$A(t) = \sum_{x \neq y} a_{xy} N_{xy}(t),$$

where a_{xy} are arbitrary real numbers with $\sum |a_{xy}| > 0$, and $N_{xy}(t)$ are the elementary *fluxes* (the number of jumps from x to y up to time t). For a time-integrated current $a_{xy} = -a_{yx}$, while for counting observables (such as the activity), $a_{xy} = a_{yx}$.

The fluctuations of $A(t)$ in the long time satisfy the following theorems [36]: (i) Strong law of large numbers, $\lim_{t\to+\infty} t^{-1} A(t) = \langle a \rangle_\pi := \sum_{x\neq y} \pi_x w_{xy} a_{xy}$ (holds almost surely). (ii) Central limit theorem (small deviations; holds in distribution) $\lim_{t\to+\infty} t^{-1/2}[A(t) - t\langle a\rangle_\pi] = \mathcal{N}(0, \sigma_\infty^2)$, where $\sigma_\infty^2 = \lim_{t\to+\infty} \sigma_\nu^2(t)/t$ and $\sigma_\nu^2(t)$ is the variance of $A(t)$ if ν is the initial distribution (notice, however, that the limit does not depend on ν). (iii) Large deviation principle (LDP)

$$\mathbb{P}_\nu\left(\frac{A(t)}{t} = \langle a\rangle_\pi + \Delta a\right) \asymp e^{-tI(\Delta a)} \quad \text{for every } \Delta a \in \mathbb{R}$$

for some rate function $I\colon \mathbb{R} \to [0, +\infty]$ which in general is hard to determine and admits an explicit analytic expression only for particular models.

To state our main result we need the following quantities. In the stationary state π, the average of A per unit time is $\langle a\rangle_\pi = \sum_{x\neq y} \pi_x w_{xy} a_{xy}$, while its static approximate variance is $\langle a^2\rangle_\pi$, with $\langle a^2\rangle_\pi = \sum_{x\neq y} \pi_x w_{xy} a_{xy}^2$ (corresponding to the variance of $\sum_{x\neq y} a_{xy}\tilde{N}_{xy}$, where $\tilde{N}_{xy}$ are independent Poisson variables with intensity $\pi_x w_{xy}$). The maximum escape rate is $q = \max_x w_{xx}$, and $c = \max_{x\neq y}|a_{xy}|$ is the maximum amplitude of the coefficients that define the observable. Since we do not assume that $\mathbb{W}$ is reversible, we denote by ε the spectral gap of the symmetrization $\Re(\mathbb{W}) = (\mathbb{W} + \mathbb{W}^\dagger)/2$, where the adjoint is taken with respect to π. Finally, we recall that the dynamical activity is the observable counting the total number of jumps between configurations [29], $K(t) = \sum_{x\neq y} N_{xy}(t)$, and denote by $\langle k\rangle_\pi := \sum_{x\neq y} \pi_x w_{xy}$ its average per unit of time at stationarity.

Main results.—We now state our three main results:

($R1$) The variance $\sigma_\pi^2(t)$ of any time-integrated current or flux observable $A(t)$ in the stationary state has the general upper bound

$$\sigma_\pi^2(t) \leq t\langle a^2\rangle_\pi \left(1 + \frac{2q}{\varepsilon}\right). \tag{1}$$

Note that this is valid for trajectories of any length t.

($R2$) The distribution of $A(t)/t$ starting from an initial measure ν obeys a *concentration* bound

$$\mathbb{P}_\nu\left(\frac{A(t)}{t} \geq \langle a\rangle_\pi + \Delta a\right) \leq C(\nu) e^{-t\tilde{I}(\Delta a)}, \tag{2}$$

where $\Delta a > 0$ is the fluctuation of A away from the stationary average, and $C(\nu) := \left(\sum_x \nu_x^2/\pi_x\right)^{1/2}$ accounts for the difference between ν and the stationary π, with $C(\pi) = 1$. The bounding rate function can be written explicitly as

$$\tilde{I}(\Delta a) = \frac{\Delta a^2}{2\left(\langle k\rangle_\pi c^2 + \frac{2q\langle a^2\rangle_\pi}{\varepsilon} + \frac{5cq\Delta a}{\varepsilon}\right)}. \tag{3}$$

($R3$) The rate function for $A(t)/t$ is lower bounded by Eq. (3) for every $\Delta a > 0$, that is

$$\tilde{I}(\Delta a) \leq I(\Delta a). \tag{4}$$

($R1$)–($R3$) are extended straightforwardly to $\Delta a < 0$ by considering the observable $-A(t)$.

While the LDP describes the *asymptotic* concentration of the law of $A(t)/t$ around the limit value $\langle a\rangle_\pi$, our main contribution consists in providing an *explicit* and *simple* bound on the probability of fluctuations valid at *any time*. Table I sketches the connection between concentration bounds and large deviations, and how the latter are derived from the former.

Inverse TUR and bound on precision.—The most direct use of TURs is in bounding the precision for estimating a

TABLE I. Connection between concentration bounds and large deviations. Concentration bounds (top row) provide bounds for the tail probability of a dynamical observable $A(t)$ and holding for all time t. The box shows our main result. Large deviations (bottom row) pertain to the asymptotic behavior of the tail probability and the moment generating function, and follow from concentration bounds in the long time limit. See text for definitions and derivations.

$\mathbb{P}_\nu[A(t) \geq t(\langle a\rangle_\pi + \Delta a)]$	Eq. (9) $\leq$	$\mathbb{E}_\nu[e^{uA(t)}]e^{-tu(\langle a\rangle_\pi+\Delta a)}$	Eq. (7) $\leq$	$\boxed{C(\nu)e^{-t\{(\langle a\rangle_\pi+\Delta a)u-\tilde{\Lambda}(u)\}}}$	$\forall\ t>0$ Concentration bounds
)(Gärtner-Ellis		)(			
$e^{-t\sup_{u\geq 0}\{(\langle a\rangle_\pi+\Delta a)u-\Lambda(u)\}}$	$\leq$	$e^{t\Lambda(u)}e^{-tu(\langle a\rangle_\pi+\Delta a)}$			$t\to+\infty$ Large deviations

current from its time average over a trajectory in a nonequilibrium stationary state (NESS) π. We define the relative error ϵ_A of A as the ratio between the variance of A and its average squared multiplied by t

$$\epsilon_A^2 := t\frac{\sigma_\pi^2(t)}{\langle A\rangle_\pi^2} = \frac{\sigma_\pi^2(t)}{t\langle a\rangle_\pi^2}. \tag{5}$$

From the standard application of the TUR together with the "inverse TUR" Eq. (1) we can bound the relative error from *below and above*

$$\frac{2}{\Sigma_\pi} \leq \epsilon_A^2 \leq \frac{\langle a^2\rangle_\pi}{\langle a\rangle_\pi^2}\left(1+\frac{2q}{\varepsilon}\right), \tag{6}$$

where $\Sigma_\pi = \sum_{x\neq y}\pi_x w_{xy}\log(\pi_x w_{xy}/\pi_y w_{yx})$ is the average entropy production rate in the NESS.

The physical meaning of our new upper bound can be understood from its two factors. In contrast to the TUR, the first factor in the right-hand side of (6) contains information about the current A of interest via the static variance, $\langle a^2\rangle_\pi$. This is measurable, being the stationary mean of $S_A(t) = \sum_{x\neq y} a_{xy}^2 N_{xy}(t)$: given a (time-asymmetric) current A, there is an associated *symmetric flux* S_A whose stationary average encodes the interplay between the localization properties of the dynamics (which jumps $x \leftrightarrow y$ have larger rates $\pi_x w_{xy}$ and $\pi_y w_{yx}$, and how these are spread among all possible transitions), and the transitions relevant for A (which $x \leftrightarrow y$ have a larger $|a_{xy}|$ giving rise to larger variations in A). The first factor therefore quantifies the intuition that if larger variations of A are produced by the most (respectively, least) active jumps, we can expect A to have large (respectively, small) fluctuations.

The second factor in the right-hand side of Eq. (6) encodes overall properties of the dynamics via the ratio q/ε. The symmetrized generator corresponds to the unique equilibrium dynamics that shares key relevant features (steady state and dynamical activity) with the original dynamics [37], and its spectral structure is able to upper bound fluctuations *at all times*. A relevant case is that of dynamics with several mesostates (phases) with frequent jumps within and rare jumps between, implying metastable behavior with large fluctuations for empirical fluxes. This is captured by q/ε, with q large due to the speed of the intrastate dynamics, and ε small (and vanishing at a first-order phase transition as shown in [38]). Thus the second factor in the right-hand side of Eq. (6) quantifies the fact that fluctuations in a time-integrated current are limited by the degree of separation of timescales in the dynamics.

Examples.—As an illustration of Eqs. (4) and (6) we consider the fluctuations of currents in the four-state model of Ref. [5]. The network of elementary transitions is shown in the inset of Fig. 1. The rates are as in Ref. [5], $w_{12}=3$, $w_{13}=10$, $w_{14}=9$, $w_{21}=10$, $w_{23}=1$, $w_{24}=2$, $w_{31}=6$, $w_{32}=4$, $w_{34}=1$, $w_{41}=7$, $w_{42}=9$, and $w_{43}=5$. A current is defined by the values of the six coefficients $a_{x>y}$ which we take in the range $a_{xy}\in[-1,1]$. To perform the analysis, we construct a mesh across the space of current observables $\mathbb{T}=[-1,1]^6$ discretized with spacing 10^{-1}, with each point corresponding to a different current.

Figure 1 shows the bounds for the long-time limit rate function $I(A/t)$ for one such current $A\in\mathbb{T}$. The full (black) curve is the exact rate function. It is calculated from the "tilted" generator $\mathbb{W}_u = \sum_{x\neq y} e^{ua_{xy}}w_{xy}|x\rangle\langle y| - \sum_x w_{xx}|x\rangle\langle x|$ as follows [36]: (i) the moment generating function (MGF) of A is $Z_{\pi,t}(u) := \mathbb{E}_\pi[e^{uA(t)}] = \langle\pi|e^{t\mathbb{W}_u}|-\rangle$, where $|-\rangle = \sum_x |x\rangle$ is the "flat state"; (ii) at long times $Z_{\pi,t}(u) \asymp e^{t\Lambda(u)}$, where the limit scaled cumulant generating function (SCGF) $\Lambda(u)$ is the largest eigenvalue of $\mathbb{W}_u$; (iii) the rate function is obtained via Legendre transform, $I(a) = \sup_u[ua-\Lambda(u)]$.

The dotted (blue) curve in Fig. 1 is the usual TUR using the entropy production [5]. The dot-dashed (pink) curve is the alternative TUR which instead of Σ_π uses the average dynamical activity, $\langle k\rangle_\pi = \sum_{x\neq y}\pi_x w_{xy}$ [9,39]. Both these curves are above the true rate function, thus providing the usual lower bounds on the size of the fluctuations of A. The dashed (red) curve represents an inverse TUR which upper bounds the size of fluctuations of A at all orders, cf. Eq. (3).

Figure 2 shows the bounds (6) on the precision error (5), for all currents in $\mathbb{T}$, both at finite and infinite t. The full (black) curves are the exact error ϵ_A^2, where the first two moments of A are obtained from the first and second

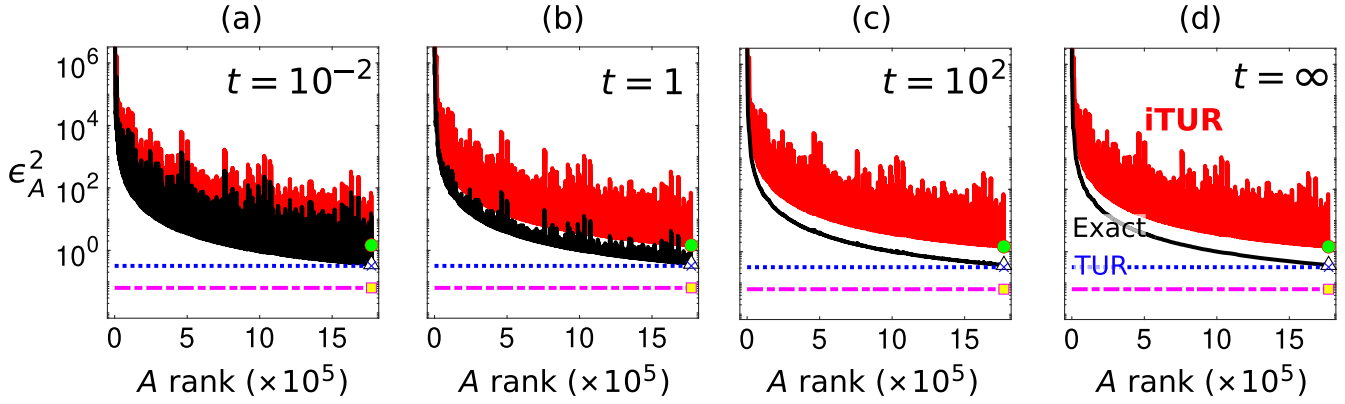

FIG. 2. Lower and upper bounds on the estimation error. (a) Relative error ϵ_A^2 for estimating a current A from a trajectory of length $t = 10^{-2}$ in the NESS of the model of Fig. 1. We show results for 20^6 different currents $A \in \mathbb{T}$. The full (black) curve is the exact error. The standard TUR, dotted (blue) line, and the activity TUR, dot-dashed (pink) line, provide lower bounds to the error which are independent of A. The inverse TUR, dashed (red) curve, gives an upper bound to the error which varies with A. (b)–(d) Same for times $t = 1, 10^2, \infty$, respectively. The data in all panels are ranked according to decreasing values of the error at $t = \infty$. For comparison, the A corresponding to entropy production is shown according to the same ranking: TUR bound (green circle), exact (white triangle), TUR (blue cross), activity TUR (yellow square).

derivatives of the MGF $Z_{\pi,t}(u)$ evaluated at $u = 0$. The errors are plotted rank ordered by their value at $t = \infty$. The dotted (blue) lines are the lower bounds from the TUR at either finite [6] or infinite [1] times. The dot-dashed (pink) lines are the activity TUR, where in the left-hand side of Eq. (6) Σ_π is replaced by $2\langle k \rangle_\pi$. As the TURs do not depend on the details of the current that they bound, these curves are constant. Figure 2 also shows the inverse TUR from the right-hand side of Eq. (6) as full (red) curves. This gives an upper bound to the error. The inverse TUR contains information about the specific current through its static average and second moment and it tracks the change in shape of the exact error: in many instances the ratio of the relative value of the upper bound to the error is smaller than that of the error to the lower bound.

As explained above, the inverse TUR captures the increase of fluctuations close to a dynamical phase transition via its dependence on q/ε, see Eq. (6). Figure 3 illustrates this in a six-state model with two competing mesostates: as the spectral gap closes with decreasing γ, the system gets trapped for longer times in each metastable phase, giving rise to larger fluctuations of currents with different mean values at stationarity in the two phases. The inverse TUR tracks this growth in the estimation error, while the TURs do not. (See Ref. [38] for details.)

Derivation of results.—We now give the main steps for the proofs of results $(R1)$–$(R3)$. For full details see Ref. [38]. Result $(R3)$ follows easily from $(R2)$ and the definition of the LDP ([38]). In order to obtain $(R1)$ and $(R2)$, the first step is upper bounding the moment generating function of $A(t)$: for every $u \geq 0$ the following holds:

$$Z_{\nu,t}(u) \leq C(\nu) e^{t\tilde{\Lambda}(u)}, \tag{7}$$

where

$$\tilde{\Lambda}(u) = \sum_{x \neq y} \pi_x w_{xy} (e^{u a_{xy}} - 1) + \frac{q \langle a^2 \rangle_\pi u^2}{\varepsilon \left(1 - \frac{5qcu}{\varepsilon}\right)} \tag{8}$$

if $0 \leq u < (\varepsilon/5qc)$, and $\tilde{\Lambda}(u) = +\infty$ otherwise. The bound (7) consists of two parts: the first summation in Eq. (8) is the SCGF of $\sum_{x \neq y} a_{xy} \tilde{N}_{xy}$, where $\tilde{N}_{xy}$ are independent Poisson random variables with rates $\pi_x w_{xy}$; the second term takes care of the correlations between the jumps of the Markov chain. $(R1)$ follows from differentiating twice Eq. (7). The Chernoff bound ([40], Sec. 2.2) allows us to turn an upper bound for the moment generating function into an upper bound for the tail probability:

$$\mathbb{P}_\nu \left(\frac{A(t)}{t} \geq \langle a \rangle_\pi + \Delta a \right) = \mathbb{P}_\nu \left(e^{uA(t)} \geq e^{tu(\langle a \rangle_\pi + \Delta a)} \right)$$
$$\leq Z_{\nu,t}(u) e^{-tu(\langle a \rangle_\pi + \Delta a)}, \quad u \geq 0. \tag{9}$$

Using Eq. (7) and optimizing in u one gets

$$\mathbb{P}_\nu \left(\frac{A(t)}{t} \geq \langle a \rangle_\pi + \Delta a \right) \leq C(\nu) e^{-t \sup_{u \geq 0} [u(\langle a \rangle_\pi + \Delta a) - \tilde{\Lambda}(u)]};$$

$(R2)$ follows from showing ([38]) that $\tilde{I}$ in (3) is dominated by the Legendre transform of $\tilde{\Lambda}$, that is

$$\tilde{I}(\Delta a) \leq \sup_{u \geq 0} [(\langle a \rangle_\pi + \Delta a) u - \tilde{\Lambda}(u)]. \tag{10}$$

The technical part consists in proving Eq. (7). As we already mentioned, a simple calculation shows that

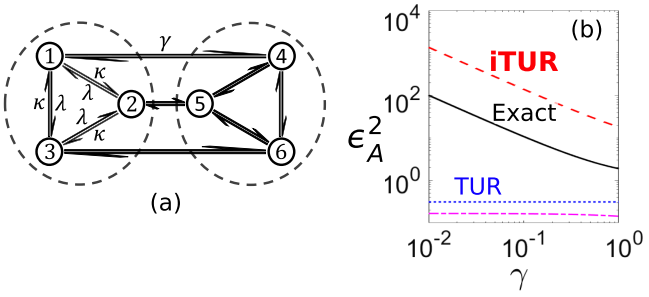

FIG. 3. Inverse TUR near metastablility. (a) Markov network of six-state model. The dashed circles indicate the two competing metastable phases at small γ. We consider $\lambda = 5$, $\kappa = 1$ while varying γ. (b) Estimation error ϵ_A^2 for the current between states 4 and 5, $A(t) = N_{45}(t) - N_{54}(t)$, as a function of γ. Full (black) curve is the exact value, upper bounded by the inverse TUR (dashed red), and lower bounded by the standard TUR (dotted blue) and the activity TUR (dot-dashed pink). Fluctuations increase with increasing metastability, which is tracked by the inverse TUR but not by the standard TUR.

$$Z_{\nu,t}(u) = \langle \nu | e^{t\mathbb{W}_u} | - \rangle, \qquad u \in \mathbb{R} \tag{11}$$

for the "tilted" generator $\mathbb{W}_u = \sum_{x \neq y} (e^{u a_{xy}} - 1) w_{xy} |x\rangle\langle y| + \mathbb{W}$, which is an analytic perturbation of $\mathbb{W}$. We consider the action of $\mathbb{W}_u$ on the inner product space of complex functions defined on the state space E endowed with the following inner product $\langle h, f \rangle_\pi = \sum_x \pi_x \bar{h}_x f_x$. Standard estimates show that

$$Z_{\nu,t}(u) \leq C(\nu) e^{t\lambda(u)},$$

where $\lambda(u) := \max\{z : z \in \mathrm{Sp}(\Re(\mathbb{W}_u))\}$. What is left is to upper bound $\lambda(u)$: for values of u small enough, perturbation theory allows us to express $\lambda(u)$ as

$$\lambda(u) = \sum_{x \neq y} \pi_x w_{xy} (e^{u a_{xy}} - 1) + \sum_{k=2}^{+\infty} u^k \lambda^{(k)}. \tag{12}$$

From the explicit expression of $\lambda^{(k)}$'s we can show that

$$|\lambda^{(k)}| \leq \frac{q \langle a^2 \rangle_\pi}{\varepsilon} \left(\frac{5qc}{\varepsilon} \right)^{k-2} \tag{13}$$

and taking u such that the geometric series converges, one gets Eq. (7) with $\tilde{\Lambda}$ given by (8).

Outlook.—We have proven a general class of upper bounds on the size of fluctuations of flux observables of trajectories which complement the lower bounds provided by TURs [41]. Results $(R1)$–$(R3)$ apply to fluctuations of all orders at all times. In contrast to standard TUR, our bounds encode details of the current of interest. Having *both* upper and lower bounds is necessary to limit the range of estimation errors.

There are many possible extensions and refinements. We focused on continuous-time Markov chains, but analogous bounds should be obtainable for discrete time dynamics. Our bounds have as input the spectral gap of the (symmetrized) generator, which for many-body systems can be estimated from time correlations [42,43]. Further approximations may also allow to formulate the inverse TURs in terms of operationally accessible quantities. The classical results here will have a corresponding generalization for open quantum dynamics by exploiting generalizations of concentration bounds to the quantum case, see, e.g., [35]. We hope to report on these extensions in future publications.

This work was supported by the EPSRC Grants No. EP/T022140/1 and No. EP/V031201/1.

[1] A. C. Barato and U. Seifert, Thermodynamic uncertainty relation for biomolecular processes, Phys. Rev. Lett. **114**, 158101 (2015).
[2] C. Maes and K. Netocny, Canonical structure of dynamical fluctuations in mesoscopic nonequilibrium steady states, Europhys. Lett. **82**, 30003 (2008).
[3] L. Bertini, A. Faggionato, and D. Gabrielli, From level 2.5 to level 2 large deviations for continuous time Markov chains, arXiv:1212.6908.
[4] L. Bertini, A. Faggionato, and D. Gabrielli, Flows, currents, and cycles for Markov chains: Large deviation asymptotics, Stoch. Proc. Appl. **125**, 2786 (2015).
[5] T. R. Gingrich, J. M. Horowitz, N. Perunov, and J. L. England, Dissipation bounds all steady-state current fluctuations, Phys. Rev. Lett. **116**, 120601 (2016).
[6] P. Pietzonka, F. Ritort, and U. Seifert, Finite-time generalization of the thermodynamic uncertainty relation, Phys. Rev. E **96**, 012101 (2017).
[7] J. M. Horowitz and T. R. Gingrich, Proof of the finite-time thermodynamic uncertainty relation for steady-state currents, Phys. Rev. E **96**, 020103(R) (2017).
[8] K. Proesmans and C. V. den Broeck, Discrete-time thermodynamic uncertainty relation, Europhys. Lett. **119**, 20001 (2017).
[9] J. P. Garrahan, Simple bounds on fluctuations and uncertainty relations for first-passage times of counting observables, Phys. Rev. E **95**, 032134 (2017).
[10] T. R. Gingrich and J. M. Horowitz, Fundamental bounds on first passage time fluctuations for currents, Phys. Rev. Lett. **119**, 170601 (2017).
[11] K. Brandner, T. Hanazato, and K. Saito, Thermodynamic bounds on precision in ballistic multiterminal transport, Phys. Rev. Lett. **120**, 090601 (2018).
[12] F. Carollo, R. L. Jack, and J. P. Garrahan, Unraveling the large deviation statistics of Markovian open quantum systems, Phys. Rev. Lett. **122**, 130605 (2019).
[13] G. Guarnieri, G. T. Landi, S. R. Clark, and J. Goold, Thermodynamics of precision in quantum nonequilibrium steady states, Phys. Rev. Res. **1**, 033021 (2019).
[14] Y. Hasegawa, Quantum thermodynamic uncertainty relation for continuous measurement, Phys. Rev. Lett. **125**, 050601 (2020).

[15] P. Pietzonka, A. C. Barato, and U. Seifert, Universal bounds on current fluctuations, Phys. Rev. E **93**, 052145 (2016).
[16] M. Polettini, A. Lazarescu, and M. Esposito, Tightening the uncertainty principle for stochastic currents, Phys. Rev. E **94**, 052104 (2016).
[17] A. Dechant and S.-i. Sasa, Entropic bounds on currents in Langevin systems, Phys. Rev. E **97**, 062101 (2018).
[18] A. C. Barato, R. Chetrite, A. Faggionato, and D. Gabrielli, Bounds on current fluctuations in periodically driven systems, New J. Phys. **20**, 103023 (2018).
[19] C. Nardini and H. Touchette, Process interpretation of current entropic bounds, Eur. Phys. J. B **91**, 1 (2018).
[20] H.-M. Chun, L. P. Fischer, and U. Seifert, Effect of a magnetic field on the thermodynamic uncertainty relation, Phys. Rev. E **99**, 042128 (2019).
[21] T. Koyuk and U. Seifert, Operationally accessible bounds on fluctuations and entropy production in periodically driven systems, Phys. Rev. Lett. **122**, 230601 (2019).
[22] T. Koyuk and U. Seifert, Thermodynamic uncertainty relation for time-dependent driving, Phys. Rev. Lett. **125**, 260604 (2020).
[23] L. P. Fischer, H.-M. Chun, and U. Seifert, Free diffusion bounds the precision of currents in underdamped dynamics, Phys. Rev. E **102**, 012120 (2020).
[24] A. Dechant and S.-i. Sasa, Fluctuation-response inequality out of equilibrium, Proc. Natl. Acad. Sci. U.S.A. **117**, 6430 (2020).
[25] K. Liu, Z. Gong, and M. Ueda, Thermodynamic uncertainty relation for arbitrary initial states, Phys. Rev. Lett. **125**, 140602 (2020).
[26] J. M. Horowitz and T. R. Gingrich, Thermodynamic uncertainty relations constrain non-equilibrium fluctuations, Nat. Phys. **16**, 15 (2020).
[27] J. P. Garrahan, R. L. Jack, V. Lecomte, E. Pitard, K. van Duijvendijk, and F. van Wijland, Dynamical first-order phase transition in kinetically constrained models of glasses, Phys. Rev. Lett. **98**, 195702 (2007).
[28] V. Lecomte, C. Appert-Rolland, and F. van Wijland, Thermodynamic formalism for systems with Markov dynamics, J. Stat. Phys. **127**, 51 (2007).
[29] C. Maes, Frenesy: Time-symmetric dynamical activity in nonequilibria, Phys. Rep. **850**, 1 (2020).
[30] P. Lezaud, Chernoff-type bound for finite Markov chains, Ann. Appl. Probab. **8**, 849 (1998).
[31] P. W. Glynn and D. Ormoneit, Hoeffding's inequality for uniformly ergodic Markov chains, Stat. Probab. Lett. **56**, 143 (2002).
[32] B. Jiang, Q. Sun, and J. Fan, Bernstein's inequality for general Markov chains, arXiv:1805.10721.
[33] J. Fan, B. Jiang, and Q. Sun, Hoeffding's inequality for general Markov chains and its applications to statistical learning, J. Mach. Learn. Res. **22**, 1 (2021).
[34] T. Benoist, L. Hänggli, and C. Rouzé, Deviation bounds and concentration inequalities for quantum noises, Quantum **6**, 772 (2022).
[35] F. Girotti, J. P. Garrahan, and M. Guţă, Concentration inequalities for output statistics of quantum Markov processes, Ann. Henri Poincaré **24**, 2799 (2023).
[36] H. Touchette, The large deviation approach to statistical mechanics, Phys. Rep. **478**, 1 (2009).
[37] A. Kolchinsky, N. Ohga, and S. Ito, Thermodynamic bound on spectral perturbations, arXiv:2304.01714.
[38] See Supplemental Material at http://link.aps.org/supplemental/10.1103/PhysRevLett.131.197101 for the mathematical proofs of the main results, rigorous justifications and derivations of some technical details and a complete analysis of the model depicted in Fig. 3.
[39] I. Di Terlizzi and M. Baiesi, Kinetic uncertainty relation, J. Phys. A **52**, 02LT03 (2018).
[40] S. Boucheron, G. Lugosi, and P. Massart, *Concentration Inequalities: A Nonasymptotic Theory of Independence* (Oxford University Press, New York, 2013).
[41] An upper bound on particle current fluctuations appeared in [15], valid only in the long time limit, for the specific case of a unicyclic network for which the moment generating function can be computed exactly.
[42] F. Noé and C. Clementi, Collective variables for the study of long-time kinetics from molecular trajectories: Theory and methods, Curr. Opin. Struct. Biol. **43**, 141 (2017).
[43] L. Bonati, G. Piccini, and M. Parrinello, Deep learning the slow modes for rare events sampling, Proc. Natl. Acad. Sci. U.S.A. **118**, e2113533118 (2021).